Research paper

Biochemical and mutational studies of allantoinase from *Bacillus licheniformis* CECT 20T

Ana Isabel Martínez-Gómez [a,b], Pablo Soriano-Maldonado [a,b],
Montserrat Andújar-Sánchez [a,b], Josefa María Clemente-Jiménez [a,b],
Felipe Rodríguez-Vico [a,b], José L. Neira [c,d], Francisco Javier Las Heras-Vázquez [a,b],
Sergio Martínez-Rodríguez [a,b,c,e,*]

[a] *Dpto. Química y Física, Universidad de Almería, Campus de Excelencia Internacional Agroalimentario, ceiA3, 04120 Almería, Spain*
[b] *Centro de Investigación en Biotecnología Agroalimentaria, BITAL, Almería, Spain*
[c] *Instituto de Biología Molecular y Celular, Universidad Miguel Hernández, 03202 Elche, Alicante, Spain*
[d] *Complex Systems Physics Institute, 50009 Zaragoza, Spain*
[e] *Dpto. Química Física, Universidad de Granada, 18071 Granada, Spain*

ARTICLE INFO

ABSTRACT

Allantoinases (allantoin amidohydrolase, E.C. 3.5.2.5) catalyze the hydrolysis of the amide bond of allantoin to form allantoic acid, in those organisms where allantoin is not the final product of uric acid degradation. Despite their importance in the purine catabolic pathway, sequences of microbial allantoinases with proven activity are scarce, and only the enzyme from *Escherichia coli* (AllEco) has been studied in detail in the genomic era. In this work, we report the cloning, purification and characterization of the recombinant allantoinase from *Bacillus licheniformis* CECT 20T (AllBali). The enzyme was a homotetramer with an apparent T_m of 62 ± 1 °C. Optimal parameters for the enzyme activity were pH 7.5 and 50 °C, showing apparent K_m and k_{cat} values of 17.7 ± 2.7 mM and 24.4 ± 1.5 s^{-1}, respectively. Co^{2+} proved to be the most effective cofactor, inverting the enantioselectivity of AllBali when compared to that previously reported for other allantoinases. The common ability of different cyclic amidohydrolases to hydrolyze distinct substrates to the natural one also proved true for AllBali. The enzyme was able to hydrolyze hydantoin, dihydrouracil and 5-ethyl-hydantoin, although at relative rates 3–4 orders of magnitude lower than with allantoin. Mutagenesis experiments suggest that S292 is likely implicated in the binding of the allantoin ring through the carbonyl group of the polypeptide main chain, which is the common mechanism observed in other members of the amidohydrolase family. In addition, our results suggest an allosteric effect of H$_2$O$_2$ toward allantoinase.

© 2013 Elsevier Masson SAS. All rights reserved.

1. Introduction

The purine catabolic pathway has been the subject of comparative biochemical studies since the early 20th century [1,2], most probably due to the interest generated by the different end products of this breakdown process, which differs among species [3, and references therein]. In fact, after a century of investigations, new outcomes appear which change established hypothesis assumed for decades [3–6]. Allantoin appears as a final/intermediate compound during purine degradation for those organisms in which uric

acid is further catabolized by the action of urate oxidase. Although during decades it has been thought that allantoin was produced by direct action of urate oxidase,[1] the appearance of only *S*-(+)-allantoin in living cells [7–9] was taken as proof of the requirement of additional enzymes for the biological conversion of uric acid [9,10]. This assumption has been recently confirmed by Ramazzina et al. [5], who have completed this catabolic pathway, explaining finally the longstanding question of how living organisms produce a single enantiomer of allantoin [6].

Allantoinases (allantoin amidohydrolase, E.C. 3.5.2.5) catalyze the hydrolysis of the amide bond of allantoin to form allantoic acid, in those organisms where allantoin is not the final product of uric

---

[1] As highlighted by Tipton [6], most biochemistry textbooks continue to present this suggestion as an established fact.

---

acid degradation. They have been widely described in plants [11–21], where allantoin has been reported to play a significant role in nitrogen metabolism for plant growth and development [21]. They have also been identified in insects [22,23], marine worms [24], amphibians [18,19,25–27] and fishes [18,19]. A comparative genomic study seems to indicate the presence of allantoinases also in non-placental mammals [4].

Allantoin degradation has also been reported in many microorganisms (see seminal work by Vogels and van der Drift [8 and references therein]). Most of the biochemical information known to date about microbial enzymes arose from studies carried out mostly during the pre-genomic era [8,9,12,15,18,19,28]. Without bioinformatic-sequence techniques, different groups of allantoin-degrading enzymes were identified based on their biochemical properties [19]. The first allantoinase sequence to be identified was that from *Saccharomyces cerevisiae* (DAL1 [29]). However, it was not till recently that Ramazzina et al. [30] described that several microorganisms able to use allantoin as a nitrogen source, lacked of any DAL1 allantoinase gene after genome sequencing; this fact drove this group to identify an alternative allantoinase gene by means of computational methods (puuE, namely metal-independent allantoinase), recruited from polysaccharide deacetylases. They confirmed the allantoinase activity of this enzyme, which does not have either significant similarity at sequence or at structural level to the DAL1 enyzme [30], and thus, they must be considered analogous enzymes.

At the structural level, DAL1 allantoinases belong to the amidohydrolase superfamily [31,32]. They present a common topology, consisting in most cases of two domains: 1) a TIM barrel, where a highly conserved bimetallic center appears; and 2) a smaller beta-sandwich, which is not present in all the members of the family [33]. Several enzymes of this superfamily are known to present broad substrate promiscuity, such as imidases [34–36], hydantoinases [33,37,38] or D-aminoacylases [39]. They are also known by a marked enantioselectivity toward their substrates [33,37–39], making them interesting candidates by their biotechnological applications [40–43]. Both the substrate promiscuity [18,19,44] and the enantioselectivity have been shown for allantoinases; although several allantoinases have been described as aspecific [12,18], the preference for the S-(+)-enantiomer has been demonstrated for several enzymes [9,12,13,18,32,45–48].

Since the electronic notation of DAL1-allantoinase sequences, low attention has been paid to microbial allantoinases. In fact, allantoinase sequences from microbial enzymes with proven activity are scarce and only that belonging to *Escherichia coli* (AllEco) has been studied in detail in the genomic era [32,44,46,49]. Strikingly, whereas the sequence similarity of the studied *E. coli* enzymes is higher than 98%, the enzymatic parameters and biophysical features reported for AllEco vary greatly among the different studied species (Table 1). Trying to provide additional data on the mechanism and enzymatic features of allantoinases, the present study reports the cloning, purification and profound characterization of the recombinant allantoinase from *Bacillus licheniformis* CECT 20T (AllBali). Based on a homology-based model and sequence analysis, we specifically altered four amino acids in the catalytic center to investigate their biochemical role in catalysis.

2. Material and methods

2.1. Materials

All chemicals were of analytical grade, and were used without further purification. TALON™ metal affinity resin was purchased from Clontech Laboratories, Inc. Allantoin and hydantoin were from Sigma, R- and S-ethylhydantoin and dihydrouracil were synthesized as described previously [33].

2.2. Microbes and culture conditions

B. licheniformis CECT 20T was used as possible donor of the allantoinase gene (*AllBali*). It was grown at 37 °C for 24 h on nutrient broth/agar I plates (1% peptone, 0.5% beef extract, 0.5% NaCl, pH 7.2, 1.5% Agar). *E. coli* DH5α was used to clone the *AllBali* gene, and *E. coli* BL21 (DE3) to overexpress the protein.

2.3. Cloning and sequence analysis of AllBali

A single-colony isolate of *B. licheniformis* CECT 20T was chosen for DNA extraction by a boiling procedure. A sample of the supernatant containing genomic DNA (5 μl) was used to amplify the gene encoding the allantoinase by PCR. The primers used were designed based on GenBank sequence accession number NC_006270, gene "*pucH*" (locus tag BL01094). These were AllBali5 (5′-CATATGAATTTTGATTCAATTATCA-3′) and AllBali3 (5′-CTCGAGGGATCCACGCGGAACCAGAGGAATAAATCTTCCTACTTT-3′), including *Nde*I and *Xho*I restriction sites, respectively. The latter also included a thrombin recognition site. The PCR fragment obtained was purified from agarose gel using QIAquick (Qiagen) and subcloned using a StrataClone™ PCR Cloning Kit (Stratagene). The isolated subcloning plasmid was purified using QIAprep Spin miniprep kit (Qiagen), and then digested using *Nde*I and *Xho*I. The digested fragment was purified from agarose gel using QIAquick (Qiagen) and then ligated into pET22b + plasmid (Novagen) cut with the same enzymes to create plasmid pAMG31. The resulting construction allows the production of the recombinant AllBali with a C-terminal polyhistidine tag (His$_6$-tag), which can be removed by thrombin cleavage.

Once the fragment had been cloned, it was sequenced using the dye dideoxy nucleotide sequencing method in an ABI 377 DNA Sequencer (Applied Biosystems). The sequence was aligned and compared with all the available amino acid sequences using the Basic Local Alignment Search Tool (BLAST [50]). Clustal W-XXL [51] was used for alignment and TREEVIEW [52] program was used to produce an unrooted phylogenetic tree.

2.4. Expression of AllBali

The *E. coli* BL21 (DE3) strain containing pAMG31 was grown in LB medium supplemented with 100 μg ml^{-1} of ampicillin. A single colony was transferred into 10 ml of LB medium with ampicillin at the above-mentioned concentration in a 100 ml flask. This culture was incubated overnight at 37 °C with shaking. 500 ml of LB supplemented with 100 μg ml^{-1} of ampicillin were inoculated with 5 ml of the overnight culture in a 2 l flask. After 2 h of incubation at 37 °C with vigorous shaking, the OD$_{600}$ of the resulting culture was 0.3–0.5. For expression induction of the *AllBali* gene, isopropyl-β-thio-D-galactopyranoside (IPTG) was added to a final concentration of 0.2 mM and the culture was continued at 34 °C for a further 6 h. In those cases where divalent cations were added during induction, a final concentration of 0.2 mM for each metal was added. The cells were collected by centrifugation (Beckman JA2-21, 7000 g, 4 °C, 20 min), and stored at −20 °C until use.

2.5. Purification of AllBali

E. coli BL21 (DE3) pAMG31 cells were resuspended in 30 ml wash buffer (300 mM NaCl, 0.02% NaN$_3$, 50 mM sodium phosphate pH 7.0). The cell walls were disrupted in ice by sonication using a UP 200 S Ultrasonic Processor (Dr. Hielscher GmbH) for 6 periods of

Table 1

Biochemical parameters of different allantoinases: (a) bacterial enzymes; (b) eukaryotic enzymes.

Organism	Opt. pH	Opt. T[a]	Thermal stability	Mol. Mass.	K_m (mM)	V_{max}/k_{cat}	Stereospecificity/stereoselectivity	Substrates	Ref.
Bacterial enzymes									
Saccharomyces cerevisiae	7–8.	<40 °C	<55 °C (pH 7, 20 min)		30		Only one optical isomer of racemic All served as a substrate		[12]
Streptococcus allantoicus	7–8		<55 °C (5 min, ≈50% r.a.)		4.9		Degradation (+)/(−)-All forms = 1; aspecific	Met-All, A-Hyd	[18] [a]
Arthrobacter allantoicus	8–8.5		<55 °C (5 min, ≈20% r.a.)		14		Degradation (+)/(−)-All forms = 1; aspecific	Met-All, A-Hyd	[18] [a]
Escherichia coli	8–8.5		<55 °C (5 min, ≈20% r.a.)		22		Degradation (+)/(−)-All forms = 1; aspecific	Met-All	[18] [a]
Escherichia coli K-12 der.	7.5–8.0	40–45 °C		52 kDa (SDS-PAGE) 200–230 kDa (GF)	4.2	6.7 mmol min^{-1} mg^{-1}		Ip-Hyd, Hyd	[44]
Escherichia coli K-12 strain W3110	7.0–8.0 (Zn^{2+}, Co^{2+}, Ni^{2+}-forms)				17.0 (Zn^{2+}) 19.5 (Co^{2+}) 80 (Ni^{2+})	5000 min^{-1} (Zn^{2+}), 28200 min^{-1} (Co^{2+}) 200 min^{-1} (Ni^{2+})	Zn^{2+}-form consumed only half of All: enantioselective for the (+) or S-All. Co^{2+}-form consumed both isomers, but 10 times faster for (+) or S-All.	No activity with Hyd or Ac-Hyd	[46]
Escherichia coli BL21	8 (Mn^{2+}-form)	40 °C (Mn^{2+}-form)	<50 °C (30 min, Mn^{2+}-form)	49.6 kDa (aa seq); 57, 94 and 190 kDa (GF)	6.2 (Mn^{2+}) 5.5 (Co^{2+}) 9.6 (Zn^{2+}) 7.3 (Ni^{2+})		Racemic All totally consumed, reaction progress curves linear, suggesting non-stereospecificity	No activity with Hyd, DHU, PHT, dHyd, 3-imo (Mn /Co-forms)	[49]
Rhizobium sp.	7.5			166 kDa (PAGE)	4.16				[15]
Pseudomonas fluorescens[b]	8–8.5		<55 °C (5 min, ≈40% r.a.)		35		Degradation (+)/(−)-All forms = 6.3	Met-All	[18] [a]
Pseudomonas acidovorans[b]	8–8.5		<55 °C (5 min, ≈20% r.a.)		45		Degradation (+)/(−)-All forms = 21.5	Met-All	[18] [a]
Pseudomonas aeruginosa[b]	8.4		<50 °C	38 kDa (SDS-PAGE) 140–150 (PAGE, GF)	5 mM S(+)-All.	1 mmol min^{-1} mg^{-1}			[28]

Organism	Opt. pH	Opt. T[a]	Thermal stability	Mol. Mass.	K_m (mM)	Stereospecificity/stereoselectivity	Substrates	Ref.
Eukaryotic enzymes								
Frog	7–9		<55 °C (5 min, ≈20% r.a.)	52 kDa (SDS-PAGE)	6	Degradation (+)/(−)-All forms = 4.9	Met-All, A-Hyd	[[18] [a] [25]]
Goldfish	7–8.5		<55 °C (5 min, ≈70% r.a.)		8.4			[18] [a]
Phaseolus hysterinus	6.5–8.0		<55 °C (5 min, >90% r.a.)		46	Degradation (+)/(−)-All forms = 13.5	Met-All, A-Hyd	[18] [a]
Glycine hispida	7–8.5		<55 °C (5 min, >90% r.a.)		14	Degradation (+)/(−)-All forms = 4.4	Met-All, A-Hyd	[18] [a]
Glycine max	6.5–7.5		<85 °C 70 °C (1 h, 100% r.a.)	30 kDa (SDS-PAGE)	17.3 (seed) 24.4 (nodule)	Only one optical isomer of D,L-All served as a substrate. Specific for D-(+)-All		[11,12,20]
Arachis hypogaea	6.0 (nodule) 7.2 (root)				8.7 (nodule) 25 (root)			[14]
Phaseolus vulgaris	7.8 (IsoI) 8.1 (IsoII)	60 (IsoI) 70 (IsoII)	<70 °C (30 min 50% r.a.) 60 °C (30 min 100% r.a.)	45 kDa (IsoI, SDS-PAGE) 53 kDa (IsoI, SDS-PAGE) 42 kDa (IsoII, PAGE) 42–110 kDa (IsoII, PAGE)	59 (IsoI) 66 (IsoII)			[16]
Lathyrus sativus	7.5				2.56	Less than 5% activity towards (−)-All.		[13]
Vigna radiata	7.5 (root) 7.5 (nodule)				20.7 (root) 20.8 (nodule)			[17]

Abbreviations: All: allantoin; Met-All: methylol-allantoin; A-Hyd: 5-aminohydantoin; Hyd: Hydantoin; DHU: dihydrouracil, PHT: phthalimide, dHyd, dihydroorotate; 3-imo, 3-iminoisoindolinone, Ac-Hyd: hydantoin-5-acetic acid; Ip-Hyd: Isopropylhydantoin. r.a.: remaining activity; GF: Gel filtration.

[a] The data shown in this reference should be carefully taken into account since pUEE allantoinases could not be distinguished.

[b] These enzymes might be pUUE-allantoinases.

30 s, pulse mode 0.5 and sonic power 60%. The pellet was precipitated by centrifugation (Beckman JA2-21, 10,000 g, 4 °C, 20 min) and discarded. The supernatant was applied to a column packed with cobalt metal affinity resin and then washed three times with wash buffer (see above). AllBali enzyme was eluted with elution buffer (100 mM NaCl, 0.02% NaN$_3$, 50 mM imidazole, 2 mM Tris, pH 8.0). Protein purity was determined at different stages of the purification by SDS-PAGE electrophoresis. An additional gel filtration chromatography step was carried out by using a Superdex 200 gel filtration column (GE Healthcare) in a BioLogic DuoFlow FPLC system (BioRad) to eliminate any DNA co-eluting with the protein, with observation at 280 nm. The purified enzyme was concentrated using an Amicon ultrafiltration system with Amicon YM-3 membranes, dialyzed against 100 mM sodium phosphate pH 7.5 and stored at 4 °C. Protein concentrations were determined from the absorbance of coefficient extinction (ε = 37,360 M^{-1} cm^{-1}) of tyrosine residues [53]. Except otherwise indicated, all experiments were conducted with cobalt-amended enzymes.

2.6. Mutation of AllBali T155, S292, D319, and K150, and purification of the resulting mutants

Mutagenesis was performed using QuikChange II Site-directed mutagenesis kit from Stratagene following the manufacturer's protocol, using the plasmid pAMG31 as template. Mutations were confirmed by using the dye dideoxy nucleotide sequencing method in an ABI 377 DNA Sequencer (Applied Biosytems). The plasmids containing the mutations (pAMG49 (T155A), pAMG50 (S292A), pAMG51 (D319N), pAMG52 (D319A), pAMG56 (K150R), and pAMG57 (T155Y)) were transformed into E. coli BL21 (DE3) and protein overexpression and purification were carried out as described above for the wild-type enzyme (induced in the presence of 0.2 mM CoCl$_2$).

2.7. Molecular mass analysis

Size exclusion chromatography-HPLC (SEC-HPLC) analysis was performed to calculate the molecular mass of the cobalt-amended wild-type and mutated AllBali enzymes using a non-denatured protein Gel Filtration Standard (BioRad). The biocompatible HPLC System (Finnigan SpectraSYSTEM HPLC; Thermo) equipped with a BioSep-SEC-S2000 (Phenomenex) was equilibrated and eluted with 100 mM buffers from pH 6.0 to 8.0 at a flow rate of 0.5 ml min^{-1} and measured at 280 nm. The molecular mass of the monomeric form was estimated by sodium dodecyl sulfate polyacrylamide gel electrophoresis (SDS-PAGE) by using a low molecular weight marker kit (GE Healthcare).

Dynamic Light Scattering (DLS) measurements were carried out with Co-AllBali samples (25–70 μM in 100 mM phosphate buffer pH 7.5) on a Zetasizer nano ZS (Malvern) at 25 °C. The signal/noise was automatically optimized. The integrated control software was run to collect, process, and store light scattering data. The control software was directly used to estimate the molecular mass from the hydrodynamic radius (R_h) value.

2.8. Circular dichroism experiments

The secondary structures of Co-AllBali mutants K150R, T155A, T155Y, S292A, D319A and D319N were compared to the wild-type Co-AllBali using far-UV circular dichroism (CD) spectra, recorded with a Jasco J850 CD spectrometer (Jasco Inc.) equipped with a JASCO PTC-423S/15 Peltier accessory. Experiments were acquired with a response time of 8 s, a bandwidth of 1 and a step resolution of 0.2 nm. Protein concentrations were 2–6 μM in 10 mM sodium phosphate buffer pH 7.5. CD measurements were taken at 25 °C

using a 1-mm path-length cuvette. Spectra were acquired from 250 to 190 nm at a scan rate of 50 nm min^{-1}, and averaged over 5 scans.

For thermal denaturations, CD spectra were measured in 100 mM sodium phosphate buffer at pH 7.5 at a protein concentration of 5 μM in a 0.1 cm cuvette. Thermal denaturation measurements were monitored by measuring the changes in the ellipticity at 222 nm. Denaturation data were collected at a scan rate of 0.2 °C min^{-1} and the temperature was increased from 25 to 95 °C.

The thermal transitions of wild-type and Co-AllBali mutants were analyzed using a two-state model [54]. The spectral parameters were fitted directly to the following equation by non-linear least square analysis:

$$S_{obs} = \frac{S_N + S_U \exp\left(-\frac{\Delta H_{VH}}{R}\left(\frac{1}{T} - \frac{1}{T_m}\right)\right)}{1 + \exp\left(-\frac{\Delta H_{VH}}{R}\left(\frac{1}{T} - \frac{1}{T_m}\right)\right)}$$

where S_{obs} is the ellipticity at 222 nm, and $S_N = A_N + B_N T$ and $S_U = A_U + B_U T$ refer to the linear dependence of the native (N) and unfolded (U) states, which have the slopes B_N and B_U, respectively. ΔH_{VH} is the apparent change in van't Hoff enthalpy, R is the universal gas constant, T is the temperature in Kelvin and T_m is the melting temperature or the transition midpoint at which 50% of the protein is unfolded. Fitting of the data was carried out with Kaleidagraph.

2.9. Enzyme assay and protein characterization

Standard enzymatic reaction was carried out with the different forms of AllBali (cation-amended or not) (50 nM–5 μM), together with allantoin (10 mM) as substrate, in 100 mM sodium phosphate buffer (pH 7.5) in 500 μl reaction volume. The reaction mixture was incubated at 50 °C for 30 min and the reaction was stopped by retrieving an aliquot of 50 μl followed by addition of 450 μl of 1% H$_3$PO$_4$. After centrifugation, the supernatant was analyzed in a HPLC system equipped with a Luna C18(2) column (250 × 4,6 mm, 100Å, 5 μm, Phenomenex) to detect allantoin and allantoic acid. The mobile phase was 100% NaH$_2$PO$_4$ 20 mM pH 4.5, pumped at a flow rate of 0.5 ml min^{-1} and monitored at 200–210 nm. The same enzyme assay was used to determine optimum temperature and pH. The temperature range was 20–75 °C and the buffers used were 100 mM sodium citrate (pH 4.0–6.0), 100 mM sodium phosphate (pH 6.0–8.0), Tris–HCl (pH 7.5–9.0) and 100 mM glycine-NaOH (pH 8.5–10.5). Thermal stability of the enzyme was determined after 60-min preincubation at different temperatures from 20 to 75 °C, in 100 mM sodium phosphate buffer pH 7.5, followed by the standard activity assay.

Enantioselectivity of Co-AllBali toward allantoin enantiomers was assayed using CD spectroscopy, recorded with a Jasco J815 CD spectrometer (Jasco Inc.) equipped with a JASCO PTC-423S/15 Peltier accessory. Substrate specificity of the enzyme was tested with substrate analogs hydantoin, R- and S-5-ethylhydantoin and dihydrouracil using the standard activity assay described above, and increasing enzyme concentration up to 200 μM. Detection of the substrate and products of the reaction was carried out as described previously [33]. Kinetic studies of Co-AllBali were conducted using allantoin as substrate following the standard assay, with concentrations of allantoin up to 50 mM. The activity of Co-AllBali mutants was measured using the standard activity assay described above, increasing enzyme concentration up to 200 μM in those mutants where activity could not be measured.

2.10. Inhibition assays

To analyze the effect of different compounds (HQSA, acetohydroxamic acid, DTT and L-cysteine; 10 and 100 mM) on enzyme

activity, samples of Co-AllBali (45 nM) were incubated with these compounds in 100 mM sodium phosphate buffer pH 7.5 (final volume 250 μl) at 4 °C for 60 min, followed by the standard enzyme assay.

Binding experiments were carried out by intrinsic fluorescence emission. Spectra were measured at 25 °C using an FP-6500 spectrofluorimeter (Jasco Inc.) equipped with an ETC 273T Peltier accessory. All measurements were carried out at a protein concentration in the range of 0.8–1 μM in a 10 mm cuvette. Samples were excited at 280 nm.

2.11. Modeling and docking studies

Two different models of AllBali were obtained by Swiss-Model server [55], using the structures of allantoinase from *E. coli* (AllEco, PDB ID. 3E74), solved at 2.10 Å [32] and that from *Bacillus halodurans* C-125 (AllBha, PDB ID. 3HM7), solved at 2.60 Å [unpublished results]. The stereochemical geometry of the final models was validated by QMean Server [56]. Docking studies of *R*- and *S*-allantoin with AllBali models were carried out with Molegro Virtual Docker.

2.12. Nucleotide and protein sequence accession number

The nucleotide and protein sequences of allantoinase gene of *B. licheniformis* CECT 20T have been deposited in the GenBank database under the accession numbers KC109790 and AGA19457, respectively.

3. Results and discussion

3.1. Sequence analysis of AllBali

A BLASTn search with the nucleotide sequence of the allantoinase from *B. licheniformis* CECT 20T (*AllBali*) reveals 100% identity with the locus tags BLi01126 and BL01094 from *B. licheniformis* DSM 13 and ATCC 14580, respectively (GenBank acc. Nos AE017333.1 and CP000002.3). When using the translated sequence of *AllBali* to carry out a BLASTp search, the highest identity found with an allantoinase of known activity is that from *E. coli* (AllEco, GenBank acc. No, P77671, 55% similarity). Sequence and phylogenetic analysis confirms the existence of two totally different groups of allantoinases (Fig. 1 SD). Allantoinase sequences of proven (or inferred) activity [11,21–23,25,29,30,44,49,57–59] were used for

this analysis. A first group (DAL1 clan) is represented by the derivatives of DAL1, containing AllBali (Fig. 1 SD). Three branches can be distinguished, where prokaryotic (branches 1 and 2) and eukaryotic (branch 3) allantoinases are grouped, although in the latter, also microbial enzymes appear. The second group (puuE clan) is formed by members of a large family named polysaccharide deacetylase (according to protein family PFAM PF01522) containing chitooligosaccharide deacetylases, polysaccharide deacetylases, chitin deacetylases and endoxylanases; the similarity between the groups is lower than 10%. AllBali also presents a high sequence similarity (aprox. 40%) with other members of the amidohydrolase family, *i.e.* dihydropyrimidinases/hydantoinases or dihydroorotases [33,38,60]. Based on the sequence similarity found within this superfamily and in their known substrate promiscuity, we could argue that some allantoin-degrading enzymes characterized in the pre-genomic era might be different amidohydrolases.

3.2. Expression and purification of AllBali: effect of cation addition during induction of the enzyme

Based on the previous results for AllEco showing differences in its activity depending on the addition of divalent cations during the induction or after enzyme purification [32,46], we decided to initially confirm whether the activity of AllBali was dependent on the moment of the addition of different cations (Fig. 1). Addition of 0.2 mM of the chloride salts of cobalt, manganese, zinc and nickel during the induction of AllBali increased enzyme activity approximately 14.2, 4.3, 1.6 and 1.3, respectively, compared to the non-amended enzyme (Fig. 1).

On the other hand, addition of the different cations after purification of non-amended AllBali resulted in partial loss of its activity, as reported for purified or partially purified allantoinases from different sources [19,44]. Far-UV CD experiments showed that the secondary structure of purified non-amended AllBali was altered after addition of Co^{2+}, Zn^{2+} (Fig. 2A and B SD, respectively), Mn^{2+} and Ni^{2+} chloride salts. As no significant changes were detected in the far-UV spectra of non-amended and cation-amended AllBali (Fig. 2C SD), we could argue that the different cations bind directly to the purified enzyme leading to secondary structure changes which, in turn, result in loss of activity. Similar results have been observed in another TIM-barrel protein (α-isopropylmalate synthase [61]), where cations interact directly with the enzyme and induce unfolding, accompanied of the loss of its functional activity. All data together suggest that the incorporation of the cation into the enzyme occurs preferentially during protein folding.

Taking into account these results, enzyme characterization was carried out with the cobalt-amended enzyme (Co-AllBali), whose purification yielded approximately 20 mg of protein *per* liter of the recombinant *E. coli* culture. SDS-PAGE analysis indicated that Co-AllBali was over 95% pure after elution of the affinity column (Fig. 2A), with an estimated molecular mass of 51 kDa (the deduced mass from the amino acid sequence, including the His$_6$-tag, is 51163 Da). Similar values were obtained for DAL1-clan members [16,25,29,44,49], although lower molecular masses have also been reported [11,20,28] (Table 1). The relative molecular mass of non-amended and Co-AllBali in the range of pHs 6.0–8.0 was estimated to be 170–215 kDa by size exclusion chromatography in a BioSep-SEC-S2000 column, suggesting that the native form of AllBali is a tetramer (Fig. 2B). We also detected dimeric species of AllBali at very low protein concentrations (<1 μM; data not shown). DLS measurements of Co-AllBali yielded an R_h value of 5.7 ± 1.6 nm at pH 7.5, with an estimated molecular mass of 196 ± 55 kDa, thus further supporting the tetrameric species. The protein from *E. coli* K-12 also showed a homotetrameric oligomerization state [32,44]
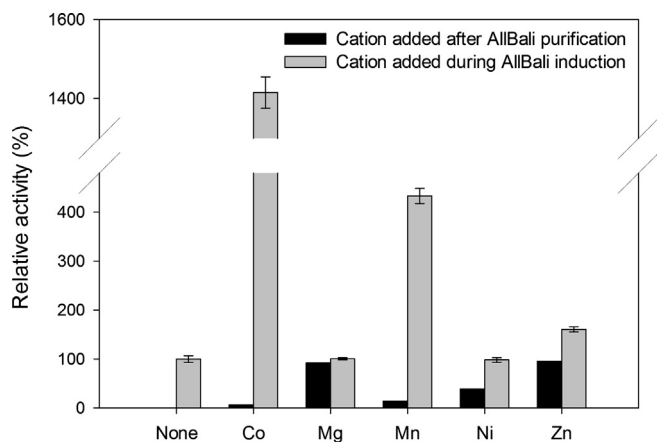

Fig. 1. Effect of different divalent cations added during the induction of AllBali (gray) or after the purification of the non-amended enzyme (black). All the values are referred to the activity found in the purified non-amended enzyme (100%).
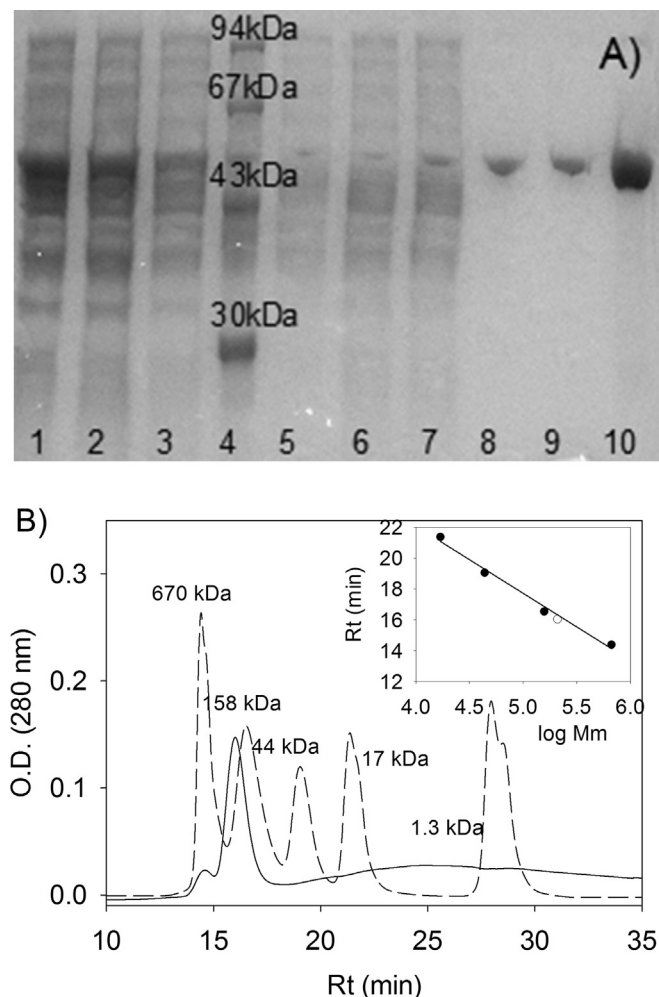
Fig. 2. A) SDS-PAGE analysis of each purification step of the recombinant allantoinase from *Bacillus licheniformis* CECT 20T (AllBali). Lanes 1 and 2, pellet and supernatant of the resuspended crude extract after cell sonication, respectively; lane 3, eluate after adding the sonicated supernatant to the metal affinity column; lane 4, low molecular weight marker; lanes 5, 6 and 7, flow-through after washing the metal affinity column with buffer; lanes 8–10, purified AllBali. B) Size Exclusion Chromatography of purified Co-AllBali at 1 mg ml^{-1} (solid line) and of the Gel Filtration Standard (BioRad, dashed line). Gel Filtration Standard: Thyroglobulin, 670 kDa; Bovine gamma-globulin, 158 kDa; Chicken ovalbumin, 44 kDa; Equine myoglobin, 17 kDa. The inset represents the fit of the retention time (R_t) *versus* the logarithm of the molecular masses of the protein standards (black circles), and that obtained for Co-AllBali (white circle), suggesting a homotetrameric native structure.

whereas that from BL21 exists as a mixture of monomers, dimers, and tetramers, in which the dimeric form is predominant [49] (Table 1). Monomeric species have been detected for *Phaseous vulgaris* enzymes [16].

3.3. Effect of pH and temperature on activity

Co-AllBali showed maximum activity at pH 7.5 (Fig. 3A SD). Similar values (7.5–8.0) have been detected for other allantoinases (Table 1) [11 and references therein, 14–16,44,49]. Lower values have been detected for allantoin degrading enzymes from peanut nodules (6.0) [14] and soybean seeds and nodules (6.5–7.5) [11]. The optimum temperature for hydrolysis of allantoin was 50 °C (Fig. 3B SD). Values ranging from 40 to 55 and 60–70 °C have been reported for *E. coli* [44,49] and *Phaseolus vulgaris* [16] allantoinases, respectively (Table 1). Thermal stability of Co-AllBali was studied by

means of two techniques: 1) pre-incubating the enzyme in 100 mM phosphate buffer (pH 7.5) at different temperatures, and subsequently measuring the residual activity with the standard assay; and 2) following the denaturation curve by means of far-UV CD. Activity was gradually lost when the enzyme was incubated at temperatures over 50 °C for 60 min (Fig. 3). Although the thermal denaturation followed by far-UV CD (Fig. 3) was irreversible, and therefore it was not possible to estimate the thermodynamic parameters governing thermal unfolding (ΔH_{vH}), we determined an apparent T_m, as has been described for other proteins showing irreversible thermal denaturations [62,63]. The T_m for Co-AllBali was 62 ± 1 °C (Table 2), which is in agreement with the results obtained measuring the residual activity after preincubation (Fig. 3). Similar results were obtained when thermal denaturation was followed by fluorescence (67 ± 1 °C, data not shown), confirming an apparent moderate thermostability of this cyclic amidohydrolase member. Whereas this is the first time that an apparent T_m has been experimentally determined for an allantoinase enzyme, similar thermal stability has been found by using other techniques for other allantoinases (Table 1) and several members of the amidohydrolase superfamily [63–66].

3.4. Effect of residues T155, S292, D319, and K150 in the activity of the enzyme

Residues K150 and D319 were mutated in order to evaluate their involvement in the bimetallic center of AllBali, since both residues are totally conserved among different cyclic amidohydrolases [33]. On the other hand, S292 and T155 residues were mutated after superposition of the modeled AllBali with the structure of *Sinorhizobium meliloti* dihydropyrimidinase (SmelDhp; PDB ID. 3DC8); the counterpart serine residue in SmelDhp (S286) is known to be involved in substrate binding, whereas T155 in the Allbali model appears in the environment where SmelDhp Y152 is located. This residue is known to assist in substrate hydrolysis [33].

Purity of the mutants was over 95% and a similar relative molecular mass to the wild-type AllBali at pH 7.5 (data not shown), showing that their oligomerization state was not altered. Far-UV CD spectra were collected to evaluate the native-like folding of the Co-amended mutants. No significant differences were found in the far-UV CD spectra of D319A and D319N mutants when compared to Co-AllBali, and then we can conclude that the secondary structure of
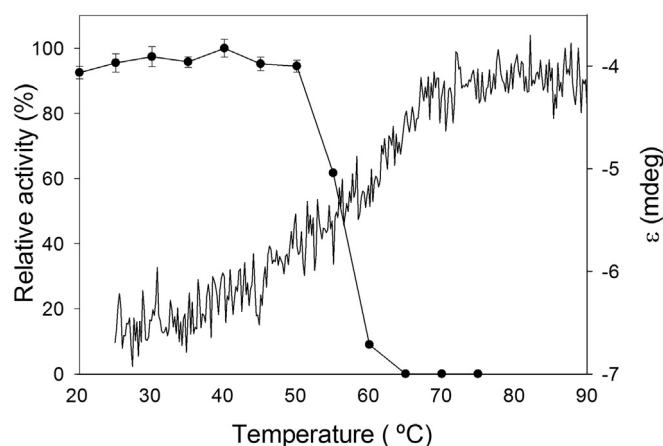

Fig. 3. CD-Thermal denaturation of Co-AllBali followed by the changes in ellipticity at 222 nm (solid line, right axis) and remaining relative activity of Co-AllBali after 30-min preincubation at the corresponding temperature (black circles, left axis). The results showing the remaining activity of Co-AllBali are the mean of three experiments, and the error bars indicate the standard deviation of the mean.

Table 2
Melting points (T_m) obtained for wild-type Co-AllBali and mutants and kinetic parameters toward allantoin.

Enzyme	T_m (°C)	K_m (mM)	k_{cat} (s^{-1})	k_{cat}/K_m (s^{-1} mM^{-1})
AllBali	62.5 ± 1.0	17.7 ± 2.7	24.4 ± 1.5	1.4 ± 0.3
T155A	61.2 ± 0.5	20.9 ± 6.3	10.1 ± 1.5	0.5 ± 0.2
T155Y	63.7 ± 1.2	20.3 ± 6.2	5.2 ± 0.7	0.3 ± 0.1
S292A	61.1 ± 0.6	35.7 ± 11.8	24.4 ± 3.0	0.7 ± 0.3
D319N	64.7 ± 0.5	–	–	–
D319A	62.2 ± 0.3	–	–	–

both mutants was the same to that of wild-type Co-AllBali; slight differences were observed for T155A, T155Y and S292A (Fig. 4 SD), which could be a result on the variation in the environment of aromatic residues according to near-UV CD spectra (data not shown). On the other hand, K150R presented a completely different far-UV spectrum (Fig. 4 SD), and therefore, we decided stop working with it. Thermal denaturations were irreversible as for the wild-type enzyme, but we determined the apparent T_m of mutants (Table 2). Mutants S292A, D319N, D319A and T155Y showed a somehow–similar transition centered in 37 °C, not observed for the wild-type enzyme nor for T155A mutant (data not shown), which might be a result of oligomerization dissociation before denaturation. Irreversibility and fitting errors did not allow obtaining reliable conclusions on the small differences observed in the T_ms among the mutants, although these results, together with the steady-state far-UV data, suggest that the mutations did not alter significantly the native-like structure.

The D319A and D319N mutants showed no detectable activity up to 200 μM of enzyme (Table 2). These results are the same as those observed previously for AllEco [32,49], confirming the role of D319 in metal-binding and/or proton shuffling. The S292A mutant showed the same k_{cat} as the wild-type enzyme, although its affinity by allantoin decreased two-fold (Table 2). Our kinetic results are in accordance to those described previously for the counterpart AllEco residue (S288 [32]). However, superposition of AllBali models and the AllEco structures with the crystallographic structures of other substrate-bound amidohydrolases (*Saccharomyces kluyveri* dihydropyrimidinase, PDB ID. 2FVK [67]; *E. coli* dihydroorotase, PDB ID. 1J79 [68]) (Fig. 5 SD) suggests a different interplay of this residue with allantoin to that suggested previously for AllEco by mean of docking experiments [32]: S292 is more likely to be implicated in the binding of the allantoin ring through the carbonyl group of the polypeptidic main chain, which is the common mechanism observed in other members of the amidohydrolase family (Fig. 5 SD) [33,67–71]. Docking studies carried out with the AllBali models and S- and R-allantoin also support our hypothesis (Fig. 6 SD). Furthermore, close evaluation of the electronic maps in the S288 environment of AllEco structure (PDB ID. E374, obtained through the EDS server) suggests an alternative conformation of this residue, which also supports this conclusion, since the carbonyl group of S288 would be flipped and orientated towards the catalytic center. This conclusion totally agrees with the suggestion on the little effect of the side-chain of this residue in enzyme activity, supported by the slight differences found in the kinetic parameters of the mutants at this serine residue (Table 2 and [32]). T155A and T155Y mutants, on the other hand, maintained approximately the same K_m as the wild-type enzyme, but decreased the k_{cat} (Table 2). Our docking results do not suggest this residue to be involved in substrate binding, and thus, the slightly lower k_{cat} might be the result of small rearrangements in the loop where this residue is placed. It is noteworthy to mention that the loop where Thr155 is place might flap upon substrate binding as has been observed in counterpart loops belonging to other members of this amidohydrolase family [70–72 and references therein].

3.5. Substrate specificity, kinetic assays and enantioselectivity of AllBali

Kinetic parameters were obtained from hyperbolic saturation curves by least-squares fit of the data to the Michaelis–Menten equation. Reactions were carried out with allantoin at different concentrations (1–50 mM) at 50 °C and pH 7.5. Under these conditions, values for the apparent K_m and k_{cat} were 17.7 ± 2.7 mM and 24.4 ± 1.5 s^{-1}, respectively (Fig. 7 SD). Other reported K_m values for allantoinases toward allantoin vary in the range of 4.16–80 mM [11,14,15,44,46,49]. The catalytic efficiency of AllBali resulted in 1.4 ± 0.3 s^{-1} mM^{-1}. The common ability of several cyclic amidohydrolases to hydrolyze different substrates [33,38,60] has also been inferred in the past for different allantoinases (Table 1) [18,44]. However, due to the difficulty in identifying whether other allantoinases, described more than 40 years ago, were DAL-1 or pUUE allantoinases [18,19], and the contradictory results found with the AllEco enzyme [18,44,46,49], we further conducted experiments to ascertain whether AllBali hydrolyzed substrates with similar chemical structure to allantoin. Co-AllBali hydrolyzed hydantoin, dihydrouracil and R- and S-5-ethyl-hydantoin (0.5 ± 0.0, 0.1 ± 0.0, 1.0 ± 0.1 and 0.1 ± 0.0 min^{-1}, respectively, Fig. 8 SD) despite using concentrations 200 times higher than for allantoin, and with relative activities 3–4 orders of magnitude lower than with the natural substrate (514.2 ± 11.2 min^{-1}). Co-AllBali was 10-fold more active for R-ethyl-hydantoin than for the S-isomer, proving its enantioselectivity toward the R-enantiomer. Thus, our results confirm that the common ability of different cyclic amidohydrolases to hydrolyze different substrates is also true for AllBali.

Studies conducted with different metal-amended forms of AllEco showed that its enantioselectivity varied in the presence of Zn^{2+} or Co^{2+}. Whereas the Zn^{2+} form was specific for S-(+)-allantoin, the cobalt form hydrolyzed both isomers, but also showing a clear preference for the (+) enantiomer [46]. Crude extracts or partially purified allantoinases from various sources are unspecific or favor the (+) isomer [9,12,13,18,32,45–48]. Whereas Co-AllBali was also able to hydrolyze completely a racemic mixture of allantoin (Fig. 4), based on its enantioselectivity toward R-5-ethylhydantoin, we wanted to unravel whether this enzyme presented an inverted enantioselectivity to that described for other allantoinases. Although we could not separate the enantiomers of allantoin by chiral-HPLC (data not shown), the appearance of a positive peak in the CD spectra during the reaction (Fig. 4, inset) proved that Co-AllBali hydrolyzed faster the R- [30,32] or (−) [7] isomer of allantoin. Previous results with AllEco suggested that the enantioselectivity of the enzyme depended on the cation appearing in the bi-metallic center [46], but as far as we know, this is the first allantoinase where a preference for the R-enantiomer has been detected. It has been previously suggested that contamination of AllEco samples with other amidohydrolase enzyme (such as hydantoinase) might be responsible for the different enantioselectivity found with the Co- and Zn-amended forms of the enzyme [46]. Thus, we wanted to unravel whether: a) the enantioselectivity; and b) the substrate promiscuity found with AllBali might be a result of the presence of a contamination with another amidohydrolase. The Co-D319A AllBali mutant activity was assayed with R- and S-5-ethyl-hydantoin using the same conditions as for Co-AllBali, but no activity was detected. These results confirm that a contamination in enzyme sample cannot account for our results, and proves the substrate promiscuity and the inverted enantioselectivity of Co-AllBali.

Whereas this is the first time that an inverted enantioselectivity of an allantoinase has been described, at least another member of the amidohydrolase superfamily has shown a similar feature (L-hydantoinase) [60]. The latter was found to be D- or L-
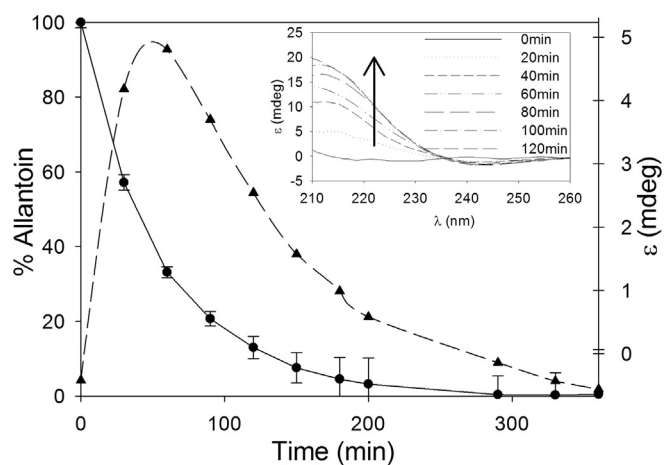
Fig. 4. Monitoring of the conversion (circles, solid line, left axis) and ellipticity (210 nm; triangles, dashed line, right axis) progresses of a racemic mixture of allantoin incubated with Co-AllBali. A 1 mM allantoin sample buffered in 100 mM phosphate (pH 7.5) was incubated with Co-AllBali (172 nM; 8.8 μg/mL) at 25 °C (750 rpm). Determination of the remaining allantoin concentration was carried out by HPLC. The presence of a positive signal during the reaction progress in the CD spectra (inset) indicates an excess of S-allantoin, showing the R-enantioselectivity of Co-AllBali.

enantioselective toward 5-methylthioethyl-hydantoin and 5-indolylmethyl-hydantoin (IMH), respectively. Docking experiments suggested that the enantioselectivity found toward L-IMH was a result of specific hydrophobic interactions generated among this specific compound with the side-chains of H62 and I95 residues [71], which are also located in the loops covering the substrate entrance of L-hydantoinase. On the other hand, since the inverted enantioselectivity of Co-AllBali arises from the presence of different cations in the bimetallic center, it is clear that our results are due to the different volume/polarizability of the Co^{2+} ion. Docking studies conducted with AllBali model (Fig. 6 SD) suggest that Asn97 and Ser321 are responsible for S-allantoin lateral chain binding as previously described [32]. The same residues might be responsible for the recognition of the ureido group of R-allantoin (Fig. 6 SD), which would explain the absence of enantioselectivity of different allantoinases. From the docking results, we can only speculate that a lower distance of the N atom of ureido group of the side-chain of S-allantoin to the metal center in the AllBali model, and to Asp319 residue (which, on the other hand, might support an enantiopreference for the S-enantiomer) (Fig. 6 SD) may in the specific case of Co-AllBali, decrease the efficiency toward the S-enantiomer due steric clashes. These steric clashes would arise from changes in the environment of the bimetallic center, thus resulting in a slight preference for the R-enantiomer. On the other hand, and taking into account the flaw of any modeling and docking experiments, we cannot rule out that changes in the environment of His61 (one of the residues conforming the bimetallic center), due to the presence of different cations, might also account for the preference of the R-enantiomer, since this residue is situated at only 3.2 Å from the side chain of the substrate in the model obtained from the docking experiments (Fig. 6 SD). Furthermore, since His61 is followed by a loop covering substrate entrance in AllBali (I62-E72) and counterpart loops are known to determine the enantiospecificity of at least D- and L-hydantoinase [70,71], we might argue that additional residue (or residues) involved in the R-enantioselectivity of Co-AllBali, not identified by the docking experiments, is (are) located in this environment. Finally, during the review process of this paper, a new work on dihydropyrimidinase from *Tetraodon nigroviridis* (another amidohydrolase family member) has confirmed our previous hypothesis on the movement of some loops covering substrate entrance of dihydropyrimidinases [33], modulated by the

presence of cations in the catalytic center [72]. Thus, by analogy with dihydropyrimidinases, the presence of different cations in the bimetallic center of allantoinase might produce unlike conformations of the counterpart loops (I62-E72 and L153-N167), resulting in the dissimilar enantioselectivity found with Co-AllBali.

3.6. Inhibition studies

The effect of different chelating and sulphydryl agents on the activity of allantoinases from different sources has been studied previously, showing very heterogeneous results (Table 1 SD). Activity of the purified AllBali enzyme decreased drastically in the presence of HQSA, acetohydroxamic acid, DTT and L-cysteine (0, 30, 0 and 0% residual activity, respectively). HQSA and acetohydroxamate inhibition is a clear result of their chelating properties, thus retrieving the cobalt present in the catalytic center. The latter was also proved to inhibit the allantoinases from *Vigna radiata* and from *Rizhobium* sp. (Table 1 SD) [15,17]. Inhibition of DTT and L-cysteine has been reported previously for other enzymes (Tables 1 and 2 SD). Whereas inhibition by DTT and L-cysteine in principle pointed toward the reduction of some disulfide bridge, inspection of the AllEco X-ray and the modeled AllBali structures did not show any S–S bond or cysteine residues close enough to form a possible disulfide bond. On the other hand, the structural information
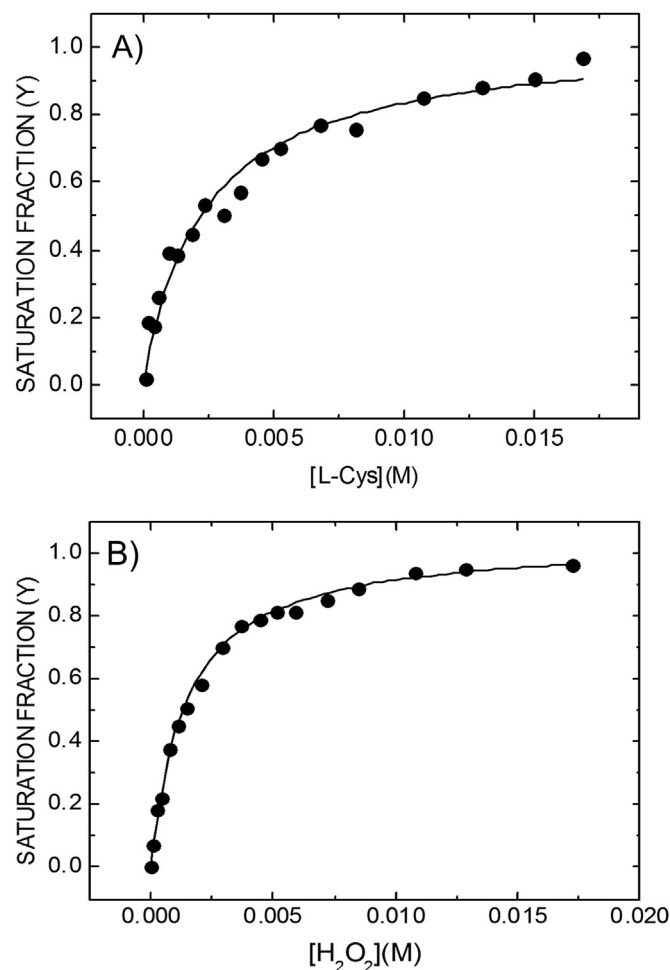

Fig. 5. Fluorescence titration of A) L-cysteine and B) H_2O_2 binding to Co-AllBali. Titrations were performed in 100 mM sodium phosphate buffer pH 7.5 and 25 °C, with enzyme concentrations of 0.8 μM. Stock ligand concentrations were 50 mM (L-cysteine) and 58.2 mM (H_2O_2).

available only suggests several cysteine residues in the environment of the catalytic cleft and/or substrate entrance (Cys151, Cys 156, Cys271 and/or Cys291) which might be affected by these reducing/oxidizing compounds. Further insights in the literature revealed that both L-cysteine [73,74] and DTT [75] can produce H_2O_2 in the reaction medium by different reactions. Therefore, we assayed the activity of the enzyme in the presence of H_2O_2, showing its ability to drastically decrease the activity of the enzyme at very low concentrations (10^{-5}%). To address whether the inhibition in the presence of both compounds was an "artifact" as a result of H_2O_2 side-production − as it has been detected in other cases [75−77], we carried out the same reaction in the presence of an excess of catalase as described [77]. Both DTT and L-cysteine inhibited similarly in the presence and absence of catalase, showing that they are inhibitors of AllBali.

Binding parameters of L-cysteine and H_2O_2 were calculated by using fluorescence, yielding affinity constants of 432.3 M^{-1} and 716.7 M^{-1}, respectively (Fig. 5). We also conducted kinetic experiments in the presence of L-cysteine and H_2O_2, using allantoin as substrate. Double-reciprocal plots showed an apparent K_i value of 0.84 mM for L-cysteine (Fig. 6A). On the other hand, kinetic plots

from experiments in the presence of H_2O_2 showed a sigmoidal shape (Fig. 6B), which might indicate an allosteric effect. In fact, as H_2O_2 is one of the products of the reaction of the preceding enzyme in the degradation route (uricase), a negative allosteric modulation might occur to allow for small intracellular concentrations of allantoin.

3.7. Funding

Acknowledgments

Appendix A. Supplementary data

Supplementary data related to this article can be found at http://dx.doi.org/10.1016/j.biochi.2013.12.002.

Fig. 6. Kinetics of Co-AllBali in the presence of L-cysteine and H_2O_2. A) Double reciprocal plots of the different experiments carried out in the presence of 0 mM (●), 0.5 mM (○), 1 mM (▼), and 2.5 mM (△) of L-cysteine, respectively. Co-AllBali activity was assayed at 50 °C and pH 7.5. The inset shows the plot of apparent K_m/V_{max} versus inhibitor concentration. The apparent K_i value for L-cysteine was 0.84 mM. B) Kinetic plot in the presence of H_2O_2 (0.0006%) showing the characteristic sigmoidal shape of allosteric effects.

References

[1] A. Hunter, M.H. Givens, C.M. Guion, Studies in the biochemistry of purine metabolism. I. The excretion of purine catabolites in the urine of marsupials, rodents and carnivora, J. Biol. Chem. 18 (1914) 387−401.

[2] A. Hunter, M.H. Givens, Studies in the comparative biochemsitry of purine metabolism. II. The excretion of purine catabolites in the urine of ungulates, J. Biol. Chem. 18 (1914) 403−416.

[3] A.C. Keebaugh, J.W. Thomas, The evolutionary fate of the genes encoding the purine catabolic enzymes in hominoids, birds, and reptiles, Mol. Biol. Evol. 27 (2010) 1359−1369.

[4] A.C. Keebaugh, J.W. Thomas, The genomes of the South American opossum (Monodelphis domestica) and platypus (Ornithorhynchus anatinus) encode a more complete purine catabolic pathway than placental mammals, Comp. Biochem. Physiol. Genom. Proteonomics 4 (2009) 174−178.

[5] I. Ramazzina, C. Folli, A. Secchi, R. Berni, R. Percudani, Completing the uric acid degradation pathway through phylogenetic comparison of whole genomes, Nat. Chem. Biol. 2 (2006) 144−148.

[6] P.A. Tipton, Urate to allantoin, specifically (S)-allantoin, Nat. Chem. Biol. 2 (2006) 124−125.

[7] E.J.'s Gravenmade, G.D. Vogels, C. van Pelt, Preparation, properties and absolute configuration of (-)-allantoin, Recueil des Travaux Chimiques des Pays-Bas 88 (1969) 929−939.

[8] G.D. Vogels, C. van der Drift, Degradation of purines and pyrimidines by microorganisms, Bacteriol. Rev. 40 (1976) 403−468.

[9] I. Okumura, K. Kondo, Y. Miyake, Stereospecificity of conversion of uric acid into allantoic acid by enzymes of Candida utilis, J. Biochem. 79 (1976) 1013−1019.

[10] I. Okumura, T.J. Yamamoto, Enzymic racemization of allantoin, J. Biochem. 84 (1978) 891−895.

[11] J.A. Bell, M.A. Webb, Immunoaffinity purification and comparison of allantoinases from soybean root nodules and cotyledons, Plant Physiol. 107 (1995) 435−441.

[12] K.W. Lee, A.H. Roush, Allantoinase assays and their application to yeast and soybean allantoinases, Arch. Biochem. Biophys. 108 (1964) 460−467.

[13] J. Nirmala, K.S. Sastry, The allantoinase of Lathyrus sativus, Phytochemistry 14 (1975) 1971−1973.

[14] N.V. Rao, R.S. Reddy, K.S. Sastry, Allantoinases of nodulated Arachis hypogaea, Phytochemistry 27 (1988) 693−695.

[15] N.V. Rao, R.S. Reddy, K.S. Sastry, An Inducible allantoinase and the specific toxicity of parabanic acid on allantoin utilization in a Rhizobium species, Curr. Microbiol. 20 (1990) 115−119.
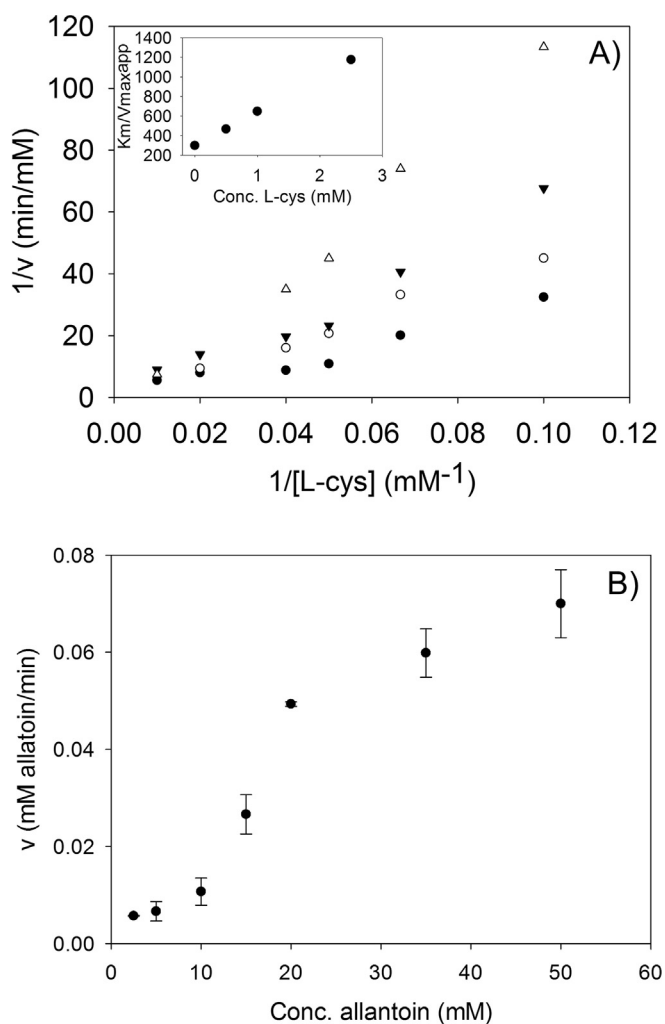
[16] M.J. Raso, M. Pineda, P. Piedras, Tissue abundance and characterization of two purified proteins with allantoinase activity from French bean (*Phaseolus vulgaris*), Physiol. Plantarum 131 (2007) 355—366.

[17] R.S. Reddy, N.V. Rao, K.S. Sastry, Acetohydroxamate, a competitive inhibitor of allantoinase of *Vigna radiata*, Phytochemistry 28 (1989) 47—49.

[18] G.D. Vogels, F. Trijbels, A. Uffink, Allantoinases from bacterial, plant and animal sources I. Purification and enzymic properties, BBA Enzymol. Biol. Oxid. 122 (1966) 482—496.

[19] G.D. Vogels, Chr. van der Drift, Allantoinases from bacterial, plant and animal sources II. Effect of bivalent cations and reducing substances on the enzymic activity, BBA Enzymol. Biol. Oxid. 122 (1966) 497—509.

[20] M.A. Webb, J.S. Lindell, Purification of allantoinase from soybean seeds and production and characterization of anti-allantoinase antibodies, Plant Physiol. 103 (1993) 1235—1241.

[21] J. Yang, K.H. Han, Functional characterization of allantoinase genes from *Arabidopsis* and a nonureide-type legume black locust, Plant Physiol. 134 (2004) 1039—1104.

[22] P.J. Gaines, L. Tang, N. Wisnewski, Insect allantoinase: cDNA cloning, purification, and characterization of the native protein from the cat flea, *Ctenocephalides felis*, Insect Biochem. Mol. Biol. 34 (2004) 203—214.

[23] P.Y. Scaraffia, G. Tan, J. Isoe, V.H. Wysocki, M.A. Wells, R.L. Miesfeld, Discovery of an alternate metabolic pathway for urea synthesis in adult *Aedes aegypti* mosquitoes, Proc. Natl. Acad. Sci. USA 105 (2008) 518—523.

[24] D.R. Passino, G.W. Brown Jr., Allantoinase in the marine polychaete *Eudistylia vancouveri*, Experientia 32 (1976) 1376—1377.

[25] S. Hayashi, S. Jain, R. Chu, K. Alvares, B. Xu, F. Erfurth, N. Usuda, M.S. Rao, S.K. Reddy, T. Noguchi, J.K. Reddy, A.V. Yeldandi, Amphibian allantoinase. Molecular cloning, tissue distribution, and functional expression, J. Biol. Chem. 269 (1994) 12269—12276.

[26] W. Masuda, S. Fujiwara, T. Noguchi, A new type of allantoinase in amphibian liver, Biosci. Biotechnol. Biochem. 65 (2001) 2558—2560.

[27] T. Noguchi, S. Fujiwara, S. Hayashi, Evolution of allantoinase and allantoicase involved in urate degradation in liver peroxisomes. A rapid purification of amphibian allantoinase and allantoicase complex, its subunit locations of the two enzymes, and its comparison with fish allantoinase and allantoicase, J. Biol. Chem. 261 (1986) 4221—4223.

[28] D.B. Janssen, R.A. Smits, C. van der Drift, Allantoinase from *Pseudomonas aeruginosa*. Purification, properties and immunochemical characterization of its *in vivo* inactivation, Biochim. Biophys. Acta 718 (1982) 212—219.

[29] R.G. Buckholz, T.G. Cooper, The allantoinase (DAL1) gene of *Saccharomyces cerevisiae*, Yeast 7 (1991) 913—923.

[30] I. Ramazzina, L. Cendron, C. Folli, R. Berni, D. Monteverdi, G. Zanotti, R. Percudani, Logical identification of an allantoinase analog (puuE) recruited from polysaccharide deacetylases, J. Biol. Chem. 283 (2008) 23295—23304.

[31] L. Holm, C. Sander, An evolutionary treasure: unification of a broad set of amidohydrolases related to urease, Proteins 28 (1997) 72—82.

[32] K. Kim, M.I. Kim, J. Chung, J.H. Ahn, S. Rhee, Crystal structure of metal-dependent allantoinase from *Escherichia coli*, J. Mol. Biol. 387 (2009) 1067—1074.

[33] S. Martínez-Rodríguez, A.I. Martínez-Gómez, J.M. Clemente-Jiménez, F. Rodríguez-Vico, J.M. García-Ruíz, F.J. Las Heras-Vázquez, J.A. Gavira, Structure of dihydropyrimidinase from *Sinorhizobium meliloti* CECT4114: new features in an amidohydrolase family member, J. Struct. Biol. 169 (2010) 200—208.

[34] Y.-W. Shi, L.-F. Cui, J.-M. Yuan, Gene cloning, expression, and substrate specificity of an imidase from the strain *Pseudomonas putida* YZ-26, Curr. Microbiol. 55 (2007) 61—64.

[35] J. Ogawa, C.L. Soong, M. Honda, S. Shimizu, Imidase, a dihydropyrimidinase-like enzyme involved in the metabolism of cyclic imides, Eur. J. Biochem. 243 (1997) 322—327.

[36] T.M. Su, Y.S. Yang, Identification, purification, and characterization of a thermophilic imidase from pig liver, Protein Expr. Purif. 19 (2000) 289—297.

[37] J.H. Chung, J.H. Back, J.-H. Lim, Y.I. Park, Y.S. Han, Thermostable hydantoinase from a hyperthermophilic archaeon, *Methanococcus jannaschii*, Enzyme Microb. Tech. 30 (2002) 867—874.

[38] J.M. Clemente-Jiménez, S. Martínez-Rogríguez, L. Mingorance-Cazorla, S. De La Escalera-Hueso, F.J. Las Heras-Vázquez, F. Rodríguez-Vico, Catalytic analysis of a recombinant D-hydantoinase from *Agrobacterium tumefaciens*, Biotechnol. Lett. 25 (2003) 1067—1073.

[39] Y.B. Yang, K.M. Hsiao, H. Li, H. Yano, A. Tsugita, Y.C. Tsai, Characterization of D-aminoacylase from *Alcaligenes denitrificans* DA181, Biosci. Biotechnol. Biochem. 56 (1992) 1392—1395.

[40] B. Wilms, A. Wiese, C. Syldatk, R. Mattes, J. Altenbuchner, Development of an *Escherichia coli* whole cell biocatalyst for the production of L-amino acids, J. Biotechnol. 86 (2001) 19—30.

[41] S. Martínez-Rodríguez, F.J. Las Heras-Vázquez, J.M. Clemente-Jiménez, L. Mingorance-Cazorla, F. Rodríguez-Vico, Complete conversion of D,L-5-monosubstituted hydantoins with a low velocity of chemical racemization into D-amino acids using whole cells of recombinant *Escherichia coli*, Biotechnol. Prog. 18 (2002) 1201—1206.

[42] A.I. Martínez-Gómez, S. Martínez-Rodríguez, J.M. Clemente-Jiménez, J. Pozo-Dengra, F. Rodríguez-Vico, F.J. Las Heras-Vázquez, Recombinant polycistronic structure of hydantoinase process genes in *Escherichia coli* for the production of optically pure D-amino acids, Appl. Environ. Microbiol. 73 (2007) 1525—1531.

[43] S. Yano, H. Haruta, T. Ikeda, T. Kikuchi, M. Murakami, M. Moriguchi, M. Wakayama, Engineering the substrate specificity of *Alcaligenes* D-aminoacylase useful for the production of d-amino acids by optical resolution, J. Chromatogr. B Analyt. Technol. Biomed. Life Sci. 879 (2011) 3247—3252.

[44] G.J. Kim, D.E. Lee, H.-S. Kim, Functional expression and characterization of the two cyclic amidohydrolase enzymes, allantoinase and a novel phenyl-hydantoinase from *Escherichia coli*, J. Bacteriol. 182 (2000) 7021—7028.

[45] G.P. Bongaerts, G.D. Vogels, Uric acid degradation by *Bacillus fastidiosus* strains, J. Bacteriol. 125 (1976) 689—697.

[46] S.B. Mulrooney, R.P. Hausinger, Metal ion dependence of recombinant *Escherichia coli* allantoinase, J. Bacteriol. 185 (2003) 126—134.

[47] F. Trijbels, G.D. Vogels, Degradation of allantoin by *Pseudomonas acidovorans*, Biochim. Biophys. Acta 113 (1966) 292—301.

[48] G.D. Vogels, Stereospecificity in the allantoin metabolism, Antonie Leeuwenhoek 35 (1969) 236—238.

[49] Y.Y. Ho, H.C. Hsieh, C.Y. Huang, Biochemical characterization of allantoinase from *Escherichia coli* BL21, Protein J. 30 (2011) 384—394.

[50] S.F. Altschul, W. Gish, W. Miller, E.W. Myers, D.J. Lipman, Basic local alignment search tool, J. Mol. Biol. 215 (1990) 403—410.

[51] M.A. Larkin, G. Blackshields, N.P. Brown, R. Chenna, P.A. McGettigan, H. McWilliam, F. Valentin, I.M. Wallace, A. Wilm, R. Lopez, J.D. Thompson, T.J. Gibson, D.G. Higgins, Clustal W and Clustal X version 2.0, Bioinformatics 23 (2007) 2947—2948.

[52] R.D. Page, TreeView: an application to display phylogenetic trees on personal computers, Comput. Appl. Biosci. 12 (1996) 357—358.

[53] S.C. Gill, P.H. von Hippel, Calculation of protein extinction coefficients from amino acid sequence data, Anal. Biochem. 182 (1989) 319—326.

[54] P.L. Privalov, Physical basis for the stability of the folded conformations of proteins, in: T.E. Creighton (Ed.), Protein Folding, W.H. Freeman & Co Ltd, New York, 1992, pp. 83—126.

[55] K. Arnold, L. Bordoli, J. Kopp, T. Schwede, The SWISS-MODEL Workspace: a web-based environment for protein structure homology modelling, Bioinformatics 22 (2006) 195—201.

[56] P. Benkert, M. Biasini, T. Schwede, Toward the estimation of the absolute quality of individual protein structure models, Bioinformatics 27 (2011) 343—350.

[57] J.L. Díaz-Leal, G. Gálvez-Valdivieso, J. Fernández, M. Pineda, J.M. Alamillo, Developmental effects on ureide levels are mediated by tissue-specific regulation of allantoinase in *Phaseolus vulgaris* L, J. Exp. Bot. 63 (2012) 4095—4106.

[58] K. Guzmán, J. Badia, R. Giménez, J. Aguilar, L. Baldoma, Transcriptional regulation of the gene cluster encoding allantoinase and guanine deaminase in *Klebsiella pneumoniae*, J. Bacteriol. 193 (2011) 2197—2207.

[59] A.C. Schultz, P. Nygaard, H.H. Saxild, Functional analysis of 14 genes that constitute the purine catabolic pathway in *Bacillus subtilis* and evidence for a novel regulon controlled by the PucR transcription activator, J. Bacteriol. 183 (2001) 3293—3302.

[60] O. May, M. Siemann, M. Pietzsch, M. Kiess, R. Mattes, C. Syldatk, Substrate-dependent enantioselectivity of a novel hydantoinase from *Arthrobacter aurescens* DSM 3745: purification and characterization as new member of cyclic amidases, J. Biotechnol. 61 (1998) 1—13.

[61] K. Singh, V. Bhakuni, Cation induced differential effect on structural and functional properties of *Mycobacterium tuberculosis* alpha-isopropylmalate synthase, BMC Struct. Biol. 7 (2007) 39.

[62] M.L. Galisteo, P.L. Mateo, J.M. Sánchez-Ruiz, Kinetic study on the irreversible thermal denaturation of yeast phosphoglycerate kinase, Biochemistry 30 (1991) 2061—2066.

[63] S. Martínez-Rodríguez, J.A. Encinar, E. Hurtado-Gómez, J. Prieto, J.M. Clemente-Jiménez, F.J. Las Heras-Vázquez, F. Rodríguez-Vico, J.L. Neira, Metal-triggered changes in the stability and secondary structure of a tetrameric dihydropyrimidinase: a biophysical characterization, Biophys. Chem. 139 (2009) 42—52.

[64] D.T. Huang, J. Kaplan, R.I. Menz, V.L. Katis, R.G. Wake, F. Zhao, R. Wolfenden, R.I. Christopherson, Thermodynamic analysis of catalysis by the dihydroorotases from hamster and *Bacillus caldolyticus*, as compared with the uncatalyzed reaction, Biochemistry 45 (2006) 8275—8283.

[65] A. Németh, S. Kamondi, A. Szilágyi, C. Magyar, Z. Kovári, P. Závodszky, Increasing the thermal stability of cellulase C using rules learned from thermophilic proteins: a pilot study, Biophys. Chem. 96 (2002) 229—241.

[66] C. Roodveldt, D.S. Tawfik, Directed evolution of phosphotriesterase from *Pseudomonas diminuta* for heterologous expression in *Escherichia coli* results in stabilization of the metal-free state, Protein Eng. Des. Sel. 18 (2005) 51—58.

[67] B. Lohkamp, B. Andersen, J. Piskur, D. Dobritzsch, The crystal structures of dihydropyrimidinases reaffirm the close relationship between cyclic amidohydrolases and explain their substrate specificity, J. Biol. Chem. 281 (2006) 13762—13776.

[68] J.B. Thoden, G.N. Phillips Jr., T.M. Neal, F.M. Raushel, H.M. Holden, Molecular structure of dihydroorotase: a paradigm for catalysis through the use of a binuclear metal center, Biochemistry 40 (2001) 6989—6997.

[69] S.H. Liaw, S.J. Chen, T.P. Ko, C.S. Hsu, C.J. Chen, A.H. Wang, Y.C. Tsai, Crystal structure of D-aminoacylase from *Alcaligenes faecalis* DA1. A novel subset of amidohydrolases and insights into the enzyme mechanism, J. Biol. Chem. 278 (2003) 4957—4962.

[70] Y.-H. Cheon, H.-S. Kim, K.-H. Han, J. Abendroth, K. Niefind, D. Schomburg, J. Wang, Y. Kim, Crystal structure of D-hydantoinase from *Bacillus stearothermophilus*: insight into the stereochemistry of enantioselectivity, Biochemistry 41 (2002) 9410—9417.

[71] J. Abendroth, K. Niefind, O. May, M. Siemann, C. Syldatk, D. Schomburg, The structure of L-hydantoinase from *Arthobacter aurescens* leads to an understanding of dihydropyrimidinase substrate and enantiospecificity, Biochemistry 41 (2002) 8589—8597.

[72] Y.C. Hsieh, M.C. Chen, C.C. Hsu, S.I. Chan, Y.S. Yang, C.J. Chen, Crystal structures of vertebrate dihydropyrimidinase and complexes from *Tetraodon nigroviridis* with lysine carbamylation: metal and structural requirements for post-translational modification and function, J. Biol. Chem. 288 (2013) 30645—30658.

[73] K.A. Nath, A.K. Salahudeen, Autoxidation of cysteine generates hydrogen peroxide: cytotoxicity and attenuation by pyruvate, Am. J. Physiol. 264 (1993) F306—F314.

[74] D.M. Miller, G.R. Buettner, S.D. Aust, Transition metals as catalysts of 'autoxidation' reactions, Free Radic. Biol. Med. 8 (1990) 95—108.

[75] P.A. Johnston, Redox cycling compounds generate H_2O_2 in HTS buffers containing strong reducing reagents-real hits or promiscuous artifacts? Curr. Opin. Chem. Biol. 15 (2011) 174—182.

[76] M.P. Bova, M.N. Mattson, S. Vasile, D. Tam, L. Holsinger, M. Bremer, T. Hui, G. McMahon, A. Rice, J.M. Fukuto, The oxidative mechanism of action of ortho-quinone inhibitors of protein-tyrosine phosphatase alpha is mediated by hydrogen peroxide, Arch. Biochem. Biophys. 429 (2004) 30—41.

[77] H. Izumi, M. Hayakari, H. Ozawa, Further studies on irreversible inhibition of dopamine-beta-hydroxylase by cysteine, Tohoku J. Exp. Med. 118 (1976) 373—380.